A unified dynamical model for plasma confinement transitions

R. Ball*

Department of Theoretical Physics, Research School of Physical Sciences & Engineering, The Australian National University, Canberra ACT 0200 Australia

(Dated: Submitted to Physical review Letters November 24, 2004)

The first smooth path, free of pathological and persistent degenerate singularities, is traversed through a dynamical model for gradient-driven, turbulence–shear flow energetics in magnetized fusion plasmas. The physics corresponding to a trapped singularity is diagnosed, and domains of fivefold multiplicity are mapped. A direct potential to shear flow energy conversion channel achieves unification of previous disparate models. The rich bifurcation and stability structure provides new intelligence on turbulence suppression, and suggests design and optimization strategies for experiments.

PACS numbers: 52.30.-q, 52.55-s, 89.75.Fb

In this work two different views of the physics behind plasma confinement transitions are smoothly reconciled in a unified model for the coupled dynamics of potential energy, turbulent kinetic energy, and shear flow kinetic energy subsystems.

Magnetized fusion plasmas are strongly driven nonequilibrium systems in which the kinetic energy of small-scale turbulence can drive the formation of large-scale coherent structures such as shear and zonal flows. This inherent tendency to self-organise is a striking characteristic of flows where Lagrangean fluid elements see a strongly two-dimensional velocity field, and is a consequence of the inverse energy cascade [1]. The distinctive properties of quasi 2-d fluid motion are the basis of natural phenomena such as zonal structuring of planetary flows, but are generally under-exploited in technology.

In plasmas the most potentially useful effect of 2-d fluid motion is suppression of high wavenumber turbulence that degrades confinement [2], which can manifest as a dramatic enhancement of sheared poloidal or zonal flows and reduction in cross-field turbulent transport. These low- to high-confinement (L–H) transitions have been the subject of intensive investigations since the 1980s. Two major strands in the literature emerged early and have persisted, both supported by experiments: (1) They are an internal phenomenon that occurs spontaneously when the rate of upscale kinetic energy transfer exceeds the nonlinear dissipation rate [3, 4]; (2) They are due to ion orbit losses near the plasma edge or induced biasing, the resulting electric field providing a torque which drives shear flows nonlinearly [5–9].

These two different physics of confinement transitions are assimilated in this Letter in a dynamical model developed by a systematic iterative method: 1. Interrogate degenerate singularities in the simplest model; 2. Unfold the singularities in physically meaningful ways, 3. Interrogate any new singularities that appear in enhanced model; 4. Repeat steps 2 and 3 until the model is free of pathological or persistent degenerate singularities, is self-consistent, reflects observations in experiments, and is therefore predictive.

The basis is the model for confinement transitions derived and analyzed in [10]:

$$\varepsilon \frac{dP}{dt} = Q - \gamma NP \tag{1}$$

$$\frac{dN}{dt} = \gamma NP - \alpha v'^2 N - \beta N^2 \tag{2}$$

$$2\frac{dv'}{dt} = \alpha v' N - \mu(P,N)v' + \varphi, \tag{3}$$

where P is the pressure gradient potential energy, N is the turbulent kinetic energy, $F = \pm v'^2$ is the shear flow kinetic energy, Q is the power input, γ and α are conservative energy transfer rate coefficients, β is the turbulence disspation rate coefficient, $\mu(P,N) = bP^{-3/2} + aPN$ represents the neoclassical and turbulent viscosities, φ is a symmetry-breaking parameter, and ε is the thermal capacitance. The skeleton dynamical system

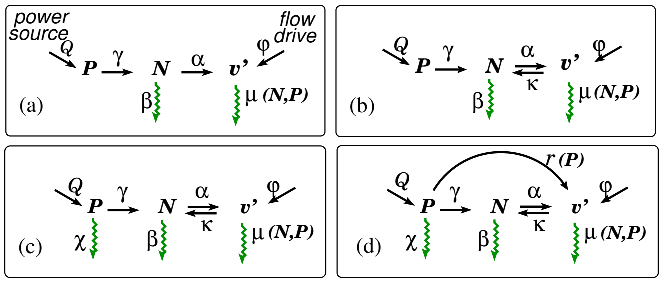

FIG. 1: Energy flux schematics for magnetized fusion plasmas. See text for explanations of each subfigure. Curly arrows indicate dissipative channels, straight arrows indicate inputs and transfers between energy-containing subsystems.

can also be written down directly by inspection of the schematic for energy flux through the P, N, and F subsystems in Fig. 1(a) and fleshed out into the model of Eqs 1–3 using the rate expressions derived in [10] and [11] from semi-empirical arguments or given as ansatzes.

The bifurcation structure of Eqs 1–3 predicts shear flow suppresion of turbulence, hysteretic, non-hysteretic, and oscillatory transitions, and saturation of the shear flow at high power input. All of these behaviors have been observed in fusion plasma systems. The model would therefore seem to be a “good” and “complete” one, in the sense of being self-consistent and expressing universally observed dynamics.

However, there are several outstanding issues that suggest the model is still incomplete. This Letter is therefore a sequel to ref. [10], in which (unusually for sequels) the most exciting and novel parts of the story are told. An inquisitive review of the bifurcation structure of Eqs 1–3 brings to light the previously unrecognized issue of trapped degenerate singularities. One of these gremlins is responsible for the unphysical prediction of infinite growth of shear flow with decreasing power input. Another issue arises from a thermal diffusivity term that was neglected in the previous work. A third issue concerns the strand (2) view of confinement transitions.I propose a unified model in which this physics is included as a direct channel between gradient potential energy and shear flow kinetic energy.

A bifurcation diagram of the equilibria of Eqs 1–3 (part of which was given in ref. [10]) is displayed in Fig. 2(a), rendered for all three dynamical variables v', P, and N,

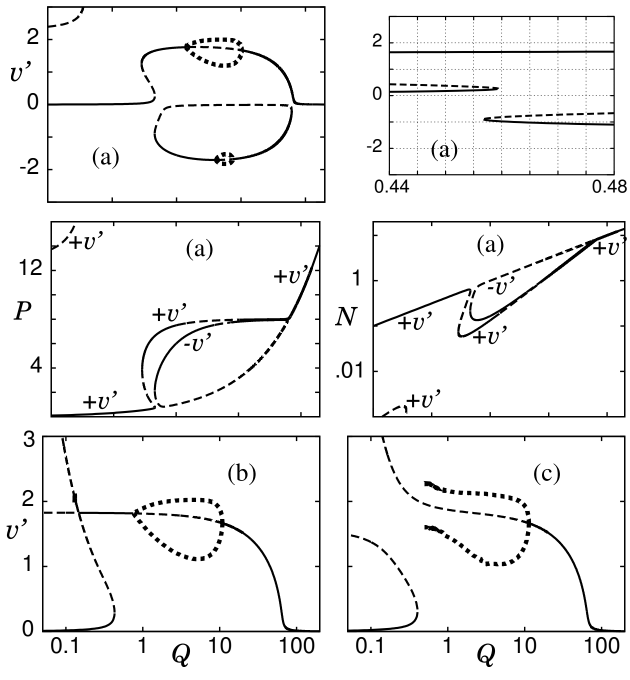

FIG. 2: (a) $\varphi = 0.05$. For clarity in the N and P renderings the limit cycle envelopes are not shown and the solution curves are annotated to indicate whether they correspond to the $+v'$ or $-v'$ domain. (b) $\varphi \approx 0.08059 = \varphi_{Tm}$. (c) $\varphi = 0.11$. Other parameters: $\beta = 1$, $b = 1$, $a = 0.3$, $\gamma = 1$, $\alpha = 2.4$, $\varepsilon = 1.5$.

with the power input Q as the control parameter. (Solid lines mark stable equilibria, dashed lines mark unstable equilibria, and amplitude envelopes of régimes of limit cycles are indicated by black dots.) I highlight two features that have particular relevance to this work.

1. The system may be evolved onto the antisymmetric, $-v'$ branch, but if the power input ebbs below the turning point at $(v', Q) \approx (-0.9, 0.46)$ the shear flow must *spontaneously* reverse direction, nominally to the lower $+v'$ branch. The zoom-in shows a small domain over which there is fivefold multiplicity comprising three stable and two unstable branches of equilibria. Two other domains of fivefold multiplicity are possible in this system, which are qualitatively different from this and from each other. They will be shown later. In the remainder of this Letter I ignore the $-v'$ régime.

2. The branch of *unstable* solutions that is just evident in the top (lower) left-hand corner leads — strangely enough — to the very heart of the model, the organizing center. For $\varphi = 0$ the bifurcation diagram features a symmetric pitchfork at $v' = 0$.But $\varphi \neq 0$ **has far-reaching global effects as well as providing a local universal unfolding of the pitchfork**, for this “new” branch of equilibria was trapped as a singularity at $(v', Q) = (\infty, 0)$ for $\varphi = 0$. As φ is increased this “new” branch begins to interact with the “old” branches and at φ_{Tm} — the organizing center — the “new” and “old” branches exchange arms, (b). In (c) a transition must still occur at the lower turning point, but classical hysteresis is (locally) forbidden. The relationship between the bifurcation structure around the organizing center and known strand (2) physics was explored in [10].

Before I pinpoint the pathology that still exists in this bifurcation structure, nonlocal to the organizing center, it is illuminating to evince the physical — or unphysical — situation by considering Eqs 1–3 on the stretched (or shrunken) timescale $\tau = t/\varepsilon$. For low thermal capacitance $\varepsilon \ll 1$ and $N \approx N_0$ and $v' \approx v'_0$. Thus the dynamics becomes quasi one-dimensional: the potential energy subsystem sees the kinetic energy dynamics as nearly constant, and $P \approx (P_0 - Q/(N_0\gamma)) \exp(-N_0\gamma\tau) + Q/(N_0\gamma)$. Reverting to real time, as $\varepsilon dP/dt \to 0$ we have $P \approx Q/(\gamma N)$; the potential energy is reciprocally slaved to the kinetic energy dynamics. The anomaly in this low-capacitance picture is that as Q ebbs the shear flow can grow quite unrealistically. In Fig. 2(c) the conjectured fate of the surviving Hopf bifurcation is a double zero eigenvalue (DZE) trap at $(Q, v') = (0, \infty)$, which is supported by extensive numerical experiments. It would seem, therefore, that some essential physics is still missing from the model.

What is not evident in Fig. 2 (because a log scale is used) is a highly degenerate branch of equilibria that exists at $Q = 0$ where $N = 0$ and $v' = (P^{3/2}\varphi)/b$; it is shown in Fig. 3(a). (Hopf bifurcations are annotated with asterisks, where limit cycle envelopes are not plotted for clarity.) For $\varphi > 0$ there is a trapped degenerate turning point, annotated as s4, where the “new” branch crosses the $Q = 0$ branch. The key to the release (or unfolding) of s4 lies in recognising that

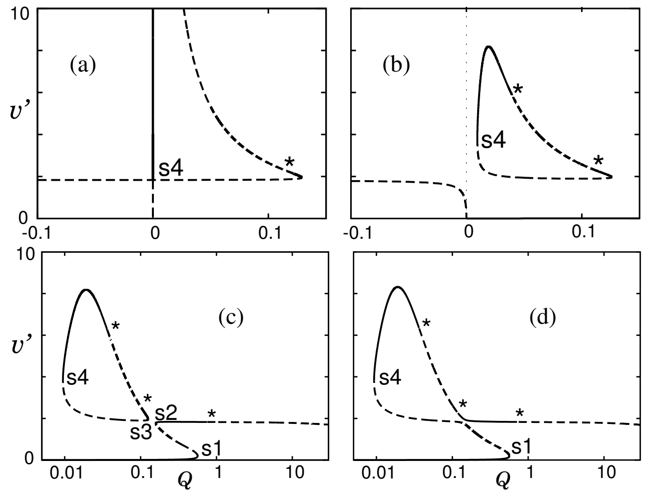

FIG. 3: (a) $\kappa = 0$, $\varphi = 0.08$; (b) $\kappa = 0.001$, $\varphi = 0.08$; (c) $\kappa = 0.001$, $\varphi = 0.083$; (d) $\kappa = 0.001$, $\varphi = 0.084$. Other parameters: $\beta = 0.3$, $b = 1$, $a = 0.3$, $\alpha = 2.4$, $\gamma = 1$, $\varepsilon = 1$.

in a flow where the velocity field is predominantly two-dimensional there will be a strong tendency to upscale energy transfer, but the net rate of energy transfer from large-scale coherent structures to high wavenumbers is not negligible [2, 12]. **What amounts to an ultraviolet catastrophe in the physics when downscale energy flux is neglected maps to a trapped degenerate singularity in the mathematical structure of the model**. A simple, conservative, back-transfer rate between the shear flow and turbulence subsystems unfolds s4 smoothly:

$$\frac{dN}{dt} = \gamma NP - \alpha v'^2 N - \beta N^2 + \kappa v'^2 \tag{4}$$

$$2\frac{dv'}{dt} = \alpha v' N - \mu(P,N)v' + \varphi - \kappa v'. \tag{5}$$

The enhanced model consists of Eqs 1, 4, and 5, and the corresponding energy flux diagram is Fig. 1(b). The back-transfer rate coefficient κ need not be identified with any particular animal in the zoo of plasma and fluid instabilities, such as the Kelvin-Helmholtz instability; it is treated simply a lumped dimensionless parameter.

The consequences of unfolding s4 can be appreciated from Fig. 3b, from which one learns a salutary lesson: unphysical equilibria and singularities should not be ignored. The unfolding creates a maximum in the shear flow and an isola of steady-state solutions, but the bifurcation diagram should be visualized as a slice of a three-dimensional surface where the third coordinate is another parameter. Two slices of this surface are shown in (c) and (d) where the other turning points are labelled s1, s2, and s3. Walking along the solution curves we make the forward transition at s1 and progress through the onset of a limit cycle régime, as in Fig. 2. This segment is henceforth designated as the *intermediate* shear flow branch, and the isola or peninsula as the *high* shear flow branch. In (c) a back-transition occurs at s2. The isola can only be reached via a transient.In (d) with diminishing Q the shear flow grows, passes through a second oscillatory régime, reaches a maximum then falls steeply; the back transition in this case occurs at s4.

The next step is to modify Eq. 1 to include a linear thermal energy dissipation rate:

$$\varepsilon\frac{dP}{dt} = Q - \gamma NP - \chi P, \tag{6}$$

where χ is a lumped dimensionless parameter that represents cross-field thermal diffusivity [13] and other non-turbulent or residual losses [14]. The model now consists of Eqs 4, 5, and 6, and in Fig. 4 a series of bifurcation

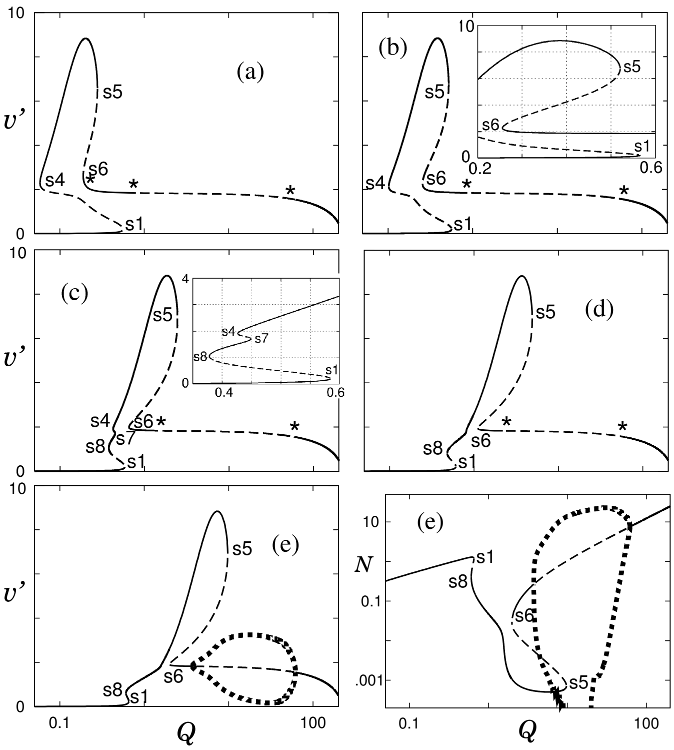

FIG. 4: (a) $\chi = 0.005$, (b) $\chi = 0.01$, (c) $\chi = 0.05$, (d) $\chi = 0.1$, (e) $\chi = 0.2$. $\kappa = 0.001$, $\varphi = 0.088$, $\beta = 0.3$, $b = 1$, $a = 0.3$, $\alpha = 2.4$, $\gamma = 1$, $\varepsilon = 1$.

diagrams has been computed for increasing values of χ. The corresponding energy schematic is Fig. 1(c).

A qualitative change is immediately apparent — the two new turning points s5 and s6 are born from a local cusp singularity — but let us begin at s1 in (b). Here, as in Fig. 3, the system jumps to an intermediate shear-flow state, but the effect of *decreasing* Q is radically different: at s6 another jump occurs to a high shear-flow state on the peninsula. Between s5 and s6 there is a domain of fivefold multiplicity, which in (c) has disappeared in a surprisingly mundane way: not through a singularity but merely by a shift of the peninsula toward higher Q. But the shift creates a *different* fivefold domain through the creation of s7 and s8 at another cusp singularity. In (d) s4 and s7 have been annihilated at yet another cusp. It is interesting and quite amusing to puzzle over the 2-parameter lines of s1, s4, s5, s6, s7, and s8 over χ projected in Fig. 5. The origins of the four cusps can be read

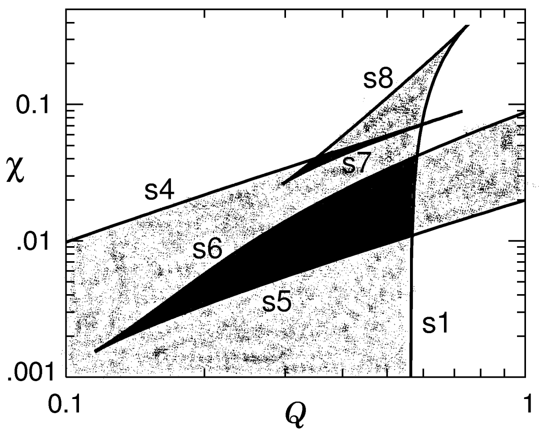

FIG. 5: In the two black areas there are five steady states and in the dusted areas there are three steady states.

off the diagram, keeping in mind that the crossovers are a *trompe de l'oeil*: they are nonlocal. At s5 in Fig. 4 (c), (d), and (e) the system transits to a limit cycle rather than to an intermediate steady state. In (e) the turbulence is enormously suppressed due to uptake of energy by the shear flow, but rises again dramatically with this hard onset of oscillations.

Finally I address the "edge electric field bifurcation" view of confinement transition physics, strand (2). The published models for this process have no coupling to the dynamics of the potential energy reservoir and turbulence. Here this physics is treated as a piece of a more holistic picture and a simple rate $r(P)$ of shear flow generation due to an ion orbit loss torque completes the model, which now consists of Eq. 4 and

$$\varepsilon\frac{dP}{dt} = Q - \gamma NP - v'^2 r(P) - \chi P \qquad (7)$$

$$2\frac{dv'}{dt} = \alpha v' N - \mu(P,N)v' + v' r(P) - \kappa v' + \varphi, \qquad (8)$$

where $r(P) = \nu \exp\left[-\left(w^2/P\right)^2\right]$. This expression simply says that the rate at which ions are lost, and hence flow is generated, is proportional to a collision frequency ν times the fraction of collisions that give ions sufficient energy to escape. The energy factor assumes a Maxwellian ion distribution and w^2 is proportional to the square of the critical escape velocity. This is the essence of expressions used by earlier authors [5–7], except that I have included explicitly the temperature dependence of r through P. The corresponding energy schematic is Fig. 1(d) where it is seen that $r(P)$ is a competing potential energy conversion channel, that can dominate the dynamics when the critical escape velocity w is low or the pressure is high.

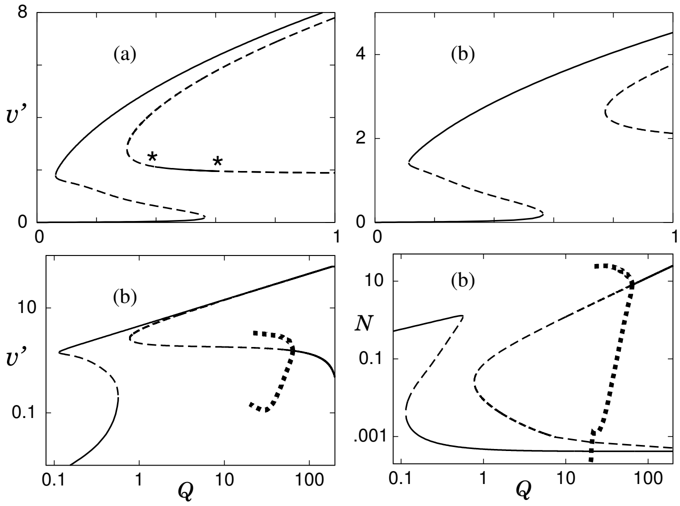

FIG. 6: (a) $\nu = 0.015$, (b) $\nu = 0.05$. $\chi = 0.01$, $\kappa = 0.001$, $\varphi = 0.088$, $\beta = 0.3$, $a = 0.3$, $\alpha = 2.4$, $b = \gamma = \varepsilon = w = 1$.

This is exactly what we see in the bifurcation diagrams, Fig. 6. The high shear-flow peninsula is elongated and flattened. The Hopf bifurcations in (a), where the $r(P)$ contribution is small, have disappeared in (b) through a DZE, leaving the intermediate branch unstable until the remaining Hopf bifurcation (c) is encountered. In the transition region the bifurcation diagram begins to look more like the simple S-shaped, cubic normal form schematics featured in numerous papers by earlier authors. However, this **unified** model accounts for shear flow suppression of the turbulence (d), whereas theirs could not.

In summary, the generation of stable shear flows and the associated confinement transitions and oscillatory behavior in magnetically contained fusion plasmas is regulated by Reynolds stress decorrelation of turbulence and/or by an induced bistable radial electric field. **These two mechanisms are unified by the first smooth path through the singularity and bifurcation structure of a dynamical model of the system**. The model is iteratively strengthened by allowing the singularities to "speak for themselves", then matching up appropriate physics to their unfoldings. These results suggest strategies for controlling access to high confinement states and manipulating oscillatory behaviour in fusion experiments. More generally I have shown that reduced dynamical models have a useful role to play in the study of one of the most formidable of complex systems, a strongly driven turbulent plasma.

This work is supported by the Australian Research Council.

---

* Electronic address: `Rowena.Ball@anu.edu.au`

[1] R. H. Kraichnan and D. Montgomery, Reports on Progress in Physics **43**, 547 (1980).
[2] P. W. Terry, Reviews of Modern Physics **72**, 109 (2000).
[3] P. H. Diamond and Y.-B. Kim, Phys. Fluids B **3**, 1626 (1991).
[4] E.-J. Kim, P. H. Diamond, and T. S. Hahm, Physics of Plasmas **11**, 4554 (2004).
[5] S.-I. Itoh and K. Itoh, Phys. Rev. Lett. **60**, 2276 (1988).
[6] K. Shaing and E. J. Crume, Phys. Rev. Lett. **63**, 2369 (1989).
[7] T. E. Stringer, Nuclear Fusion **33**, 1249 (1993).
[8] A. Fujisawa, Plasma Phys. Control. Fusion **45**, R1 (2003).
[9] S. Magni, C. Riccardi, and H. E. Roman, Physics of Plasmas **11**, 4564 (2004).
[10] R. Ball, R. L. Dewar, and H. Sugama, Phys. Rev. E **66**, 066408 (2002).
[11] H. Sugama and W. Horton, Plasma Phys. Control. Fusion **37**, 345 (1995).
[12] R. Ball, in *Encyclopedia of Nolinear Science*, edited by A. Scott (Routledge, 2004).
[13] S. I. Braginskii, in *Reviews of Plasma Physics*, edited by M. A. Leontovich (Consultants Bureau, New York, 1965), vol. 1.
[14] A. Thyagaraja, F. A. Haas, and D. J. Harvey, Physics of Plasmas **6**, 2380 (1999).